Pergamon

Tetrahedron 58 (2002) 9769–9777

TETRAHEDRON

Glycoluril derivatives form hydrogen bonded tapes rather than cucurbit[*n*]uril congeners

Anxin Wu,[a,b] James C. Fettinger[a] and Lyle Isaacs[a,*]

[a]*Department of Chemistry and Biochemistry, University of Maryland, College Park, MD 20742, USA*
[b]*National Laboratory of Applied Organic Chemistry, Lanzhou University, Lanzhou 730000, People's Republic of China*

Received 30 August 2002; revised 9 October 2002; accepted 15 October 2002

Abstract—The synthesis and X-ray crystallographic characterization of diphenylglycoluril derivatives (**1**–**4**) that possess one or two alkyl groups on their N- or O-atoms is reported. Compounds **1**–**4** preferentially form linear hydrogen bonded tapes in the crystal by heterochiral recognition processes. We do not observe cyclic hydrogen bonded cucurbit[*n*]uril congeners that would result from homochiral recognition processes. The high propensity of alkylated derivatives of diphenylglycoluril to form hydrogen bonded tapes stands in stark contrast to the reported X-ray crystal structures of other known alkylated derivatives of glycoluril. We attribute this high propensity to form tapes to the phenyl and alkyl substituents that impart good solubility in non-polar aprotic solvents which do not compete for H-bonds. These results suggest that suitably functionalized glycoluril derivatives have untapped potential in studies of crystal engineering.

1. Introduction

Glycoluril (**5**) is an important building block for both molecular and supramolecular chemistry. For example, glycoluril derivatives have been used in a variety of applications including polymer cross-linking, psychotropic agents, explosives, in the stabilization of organic compounds against photodegradation, textile waste stream purification, and combinatorial chemistry.[1] In the area of supramolecular chemistry, glycoluril derivatives have been used as the basis for molecular capsules,[2] molecular clips,[3] models of polyketide biosynthesis,[4] self-complementary facial amphiphiles,[5] xerogels,[6] and the cucurbit[*n*]uril (**CB**[*n*]) family.[7]

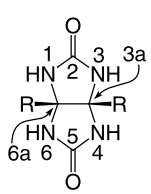

5a R = H
5b R = Me
5c R = Ph

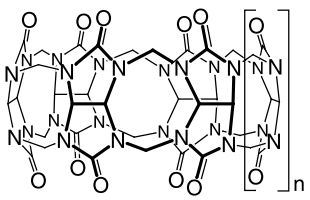

CB[5] (n = 0) **CB**[8] (n = 3)
CB[6] (n = 1) **CB**[10] (n = 5)
CB[7] (n = 2)

One area of glycoluril supramolecular chemistry that has been less well explored is its utilization as a platform for studies of crystal engineering.[8] We use Etter's graph set notation to describe the hydrogen bond motifs in this paper.[9,10] One of the most important motifs for studies of crystal engineering involves the formation of hydrogen bonded tapes. Tapes comprise linear aggregates of molecules where each molecule is hydrogen bonded to exactly two other molecules by the formation of eight-membered rings typically forming $R_2^2(8)$ H-bonding motifs. Hydrogen bonded tapes have been observed for several classes of molecules including cyanuric acid and melamine,[11] bicyclic bis-lactams,[12] diketopiperazines,[13,14] thioureas,[15] and benzimidazolene-2-thiones,[16] and has been the subject of excellent reviews.[17,18] To date, known X-ray crystal structures of compounds containing a single glycoluril ring include the parent glycoluril,[19,20] its 3a,6a derivatives,[8,21,22] nitrated derivatives,[23] molecular clips,[24] components for molecular encapsulation,[25] hexacyclic compounds,[26] acylated derivatives,[27–29] cyclic ethers,[30,31] and alkylated derivatives.[32–37] To the best of our knowledge, however, no glycoluril derivatives have been reported to form H-bonded tapes in the crystal.[38] This deficiency is particularly surprising since: (1) the well developed nature of the synthetic chemistry of glycoluril allows the preparation of a wide range of derivatives, (2) the rigid glycoluril skeleton results in derivatives with well defined geometries, (3) it is one of a small number of non-planar building blocks, and (4) many of the derivatives of glycoluril are inherently chiral due to substitution pattern alone which can lead to interesting stereochemical properties. In this paper we report that alkylated glycoluril derivatives (±)-**1**, (±)-**2**, **3**, and (±)-**4** form hydrogen bonded tapes in the crystal by heterochiral recognition processes.

Keywords: glycoluril; hydrogen bonding; tapes; cucurbituril; crystal engineering.

* Corresponding author. Tel.: +1-301-405-1884; fax: +1-301-314-9121; e-mail: li8@umail.umd.edu

0040–4020/02/$ - see front matter
PII: S0040-4020(02)01307-8

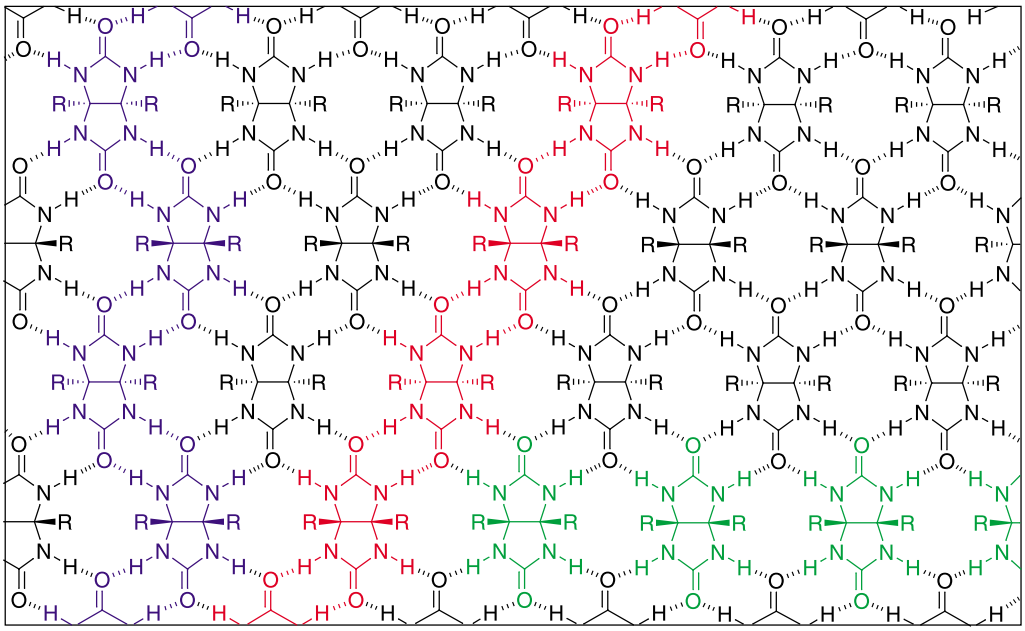

Figure 1. Schematic representation of the connectivity observed in the crystal structures of **5a** and **5b**. The blue and red highlighted regions depict two possible linear tape motifs that can be excised from the crystal lattice. The green region highlights a hypothetical tape motif formed by the side-by-side interactions of glycoluril molecules.

2. Results and discussion

2.1. Design of the molecular components for H-bonded self-assembly

Fig. 1 shows a schematic representation of the connectivity observed in the crystal structures of **5a** and **5b**. All four H-bond donating NH groups and both H-bond accepting ureidyl C═O groups become fully H-bonded through the formation of $R_2^2(8)$ motifs comprising N–H···O H-bonds. This leads to a molecular sheet in which each molecule is H-bonded to four neighboring molecules. Following the conceptual framework developed by Whitesides for crystal engineering the cyanuric acid·melamine lattice,[11,14,16] we decided to examine the crystal structure of **5a** for the presence of repetitive H-bonding tape motifs. The regions highlighted in blue and red represent two infinite tapes that might be accessible by appending substituents to the 1,6- and 1,4-positions of the glycoluril skeleton, respectively.

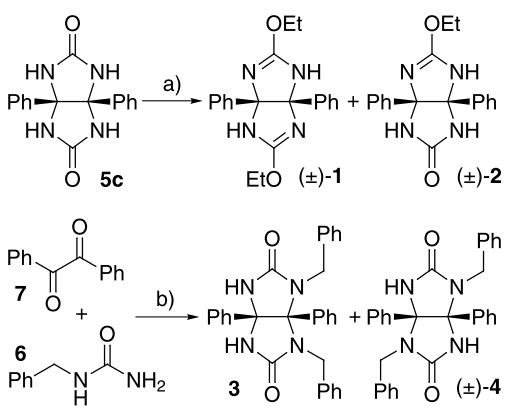

Scheme 1. Synthesis of **1**–**4**. *Conditions*: (a) Et_3OBF_4, $ClCH_2CH_2Cl$; (b) EtOH, HCl, reflux.

These substituents are intended to enforce the formation of tapes by preventing H-bonding interactions perpendicular to the tapes. We designed dibenzyl diphenyl glycoluril derivatives **3** and (±)-**4** to with this consideration in mind (Scheme 1). In particular, we chose to use phenyl and benzyl substituents on these molecules to improve their solubility characteristics in non-polar aprotic organic solvents. The use of polar protic solvents for the crystallization of related dialkyl glycoluril derivatives lead to non-tape structures.[32–34,36] A third linear tape shown in green is conceptually accessible by the transposition of two H-bond donating NH groups with the H-bond acceptor C═O groups. The enol forms of the ureidyl groups present just such a transposition. To express the H-bonding information present in the enol form, we targeted di-*O*-alkylated glycoluril derivatives. For this purpose, we prepared (±)-**1**, and as a side product obtained mono-alkylated (±)-**2** (Scheme 1).

Through our work on the chemistry and recognition properties of methylene bridged glycoluril dimers, we have become interested in the chemistry of cucurbit[*n*]uril, its derivatives, and its congeners.[39] As a secondary motivation for the synthesis and X-ray crystallographic characterization of **1** and **3**, we considered the influence of relative stereochemistry on the formation of H-bonded tapes. Tapes formed from **1** or **3**, for example, display their phenyl groups on alternate sides of the tape which leads to linear tapes. The alternative mode of aggregation, that displays the all of the phenyl groups on the same side of the tape would lead to cyclic tape-like structures $\mathbf{1}_n$ and $\mathbf{3}_n$, respectively. Compounds $\mathbf{1}_n$ and $\mathbf{3}_n$ can be considered H-bonded cucurbit[*n*]uril congeners. Such aggregates could be expected to retain some of the interesting molecular recognition properties that have been demonstrated for cucurbit[*n*]uril and molecular capsules.[2,40,41]

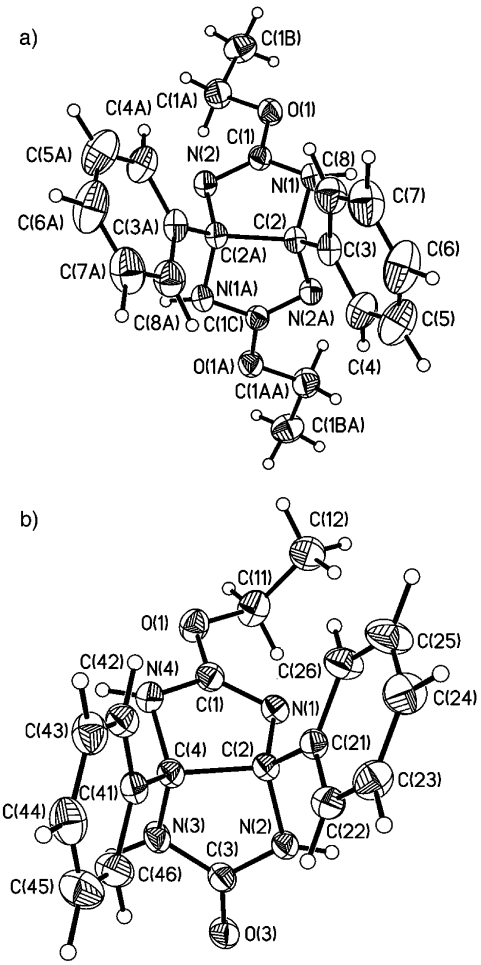

Figure 2. ORTEP plot of the molecular structures of: (a) (±)-**1** and (b) (±)-**2** in the crystal. Only one enantiomer is shown. Thermal ellipsoids are drawn at the 50% probability level.

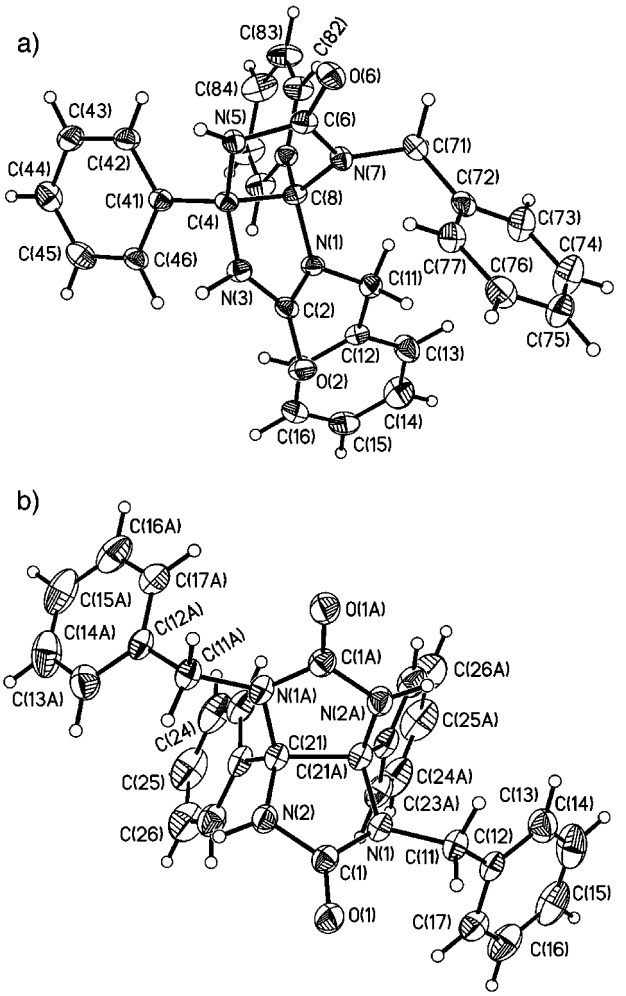

Figure 3. ORTEP plot of the molecular structures of (a) **3** and (b) (±)-**4** in the crystal. Only one enantiomer is shown. Thermal ellipsoids are drawn at the 50% probability level.

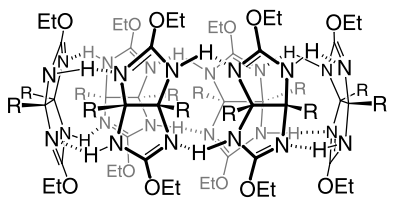

1$_n$ R = Ph

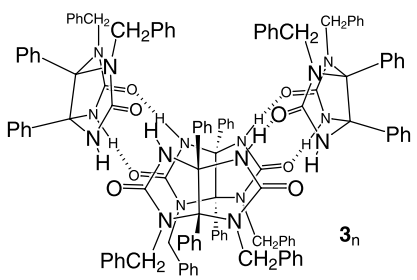

3$_n$

2.2. Synthesis of molecular components for H-bonded self-assembly

Scheme 1 shows the synthesis of **1**–**4**. Diphenyl glycoluril **5c** was ethylated with Et_3OBF_4 in $ClCH_2CH_2Cl$ to deliver (±)-**1** (5%) and (±)-**2** (22%) in modest yield.[42] Condensation of benzylurea (**6**) and benzil (**7**) in refluxing EtOH saturated with HCl yielded **3** (20%) and (±)-**4** (20%). Compound (±)-**1** is C_2 symmetric and contains two NH groups and two H-bond accepting C═N groups whereas (±)-**2** is C_1 symmetric containing three NH groups and two H-bond acceptors (C═O and C═N). Compounds **3** and (±)-**4** contain two benzyl substituents on the same, and opposite sides of the glycoluril rings, respectively. These two benzyl substituents reduce the number of hydrogen bonding ureidyl NH groups to two and while retaining both carbonyl groups as potential H-bond acceptors. Compounds **1**, **2**, and **4** are chiral; in this study we obtained and used the corresponding racemic mixtures.

2.3. Molecular structure of 1–4 as determined by X-ray crystallography

We were able to obtain single crystals of **1**–**4** by recrystallization from non-polar solvents (**1**: $CHCl_3$, **2**: CH_2Cl_2/CH_3CN and $CHCl_3$/MeOH, **3**: $CHCl_3/CH_3CN$ and CH_2Cl_2/CH_3CN, **4**: C_6H_6, $ClCH_2CH_2Cl$, and $PhCH_3$). Fig. 2 shows ORTEP plots of the molecular structures of (±)-**1** and (±)-**2** in the crystal. The structures of (±)-**1** and (±)-**2**

are similar to those reported previously for other glycoluril derivatives. Both compounds contain *cis*-fused five-membered rings bearing two phenyl groups which imparts curvature to the molecule. The mean planes through the two five-membered rings intersect with angles of 109.7° (**1**) and 109.6° (**2**). These values are somewhat smaller than those observed for dimethylated derivatives of **5a** (121.4°)[36] and **5b** (117.9°)[34] and correlates with the increase in steric bulk of the substituents on the convex face of glycoluril. The glycoluril skeletons are significantly twisted which is manifested in the dihedral angles between the ipso C-atoms of the phenyl rings and the bridgehead C-atoms (**1**: 13°) and (**2**: 22°). This twisting is commonly observed in glycoluril derivatives and has ranged from 0°[34,36] to 30.5°,[29] with values up to 24° being observed for derivatives of **5c**.[43] The intramolecular distance between the O-atoms amount to 5.46 Å (**2**) and 5.53 Å (**3**) which are in the range commonly observed for diphenyl glycoluril derivatives.[22e,i,j,39] This distance defines the potential cavity depth of the hypothetical cyclic oligomer $\mathbf{3}_n$ formed by its self-association. This cavity depth is slightly smaller than that of **CB**[6] (5.98–6.04 Å).[7b]

Fig. 3 shows the X-ray crystal structures **3** and (±)-**4**. The molecular structures of **3** and (±)-**4** are similar to those obtained for related glycoluril derivatives previously. Again, the *cis*-fused five-membered rings bearing phenyl groups enforces their cup shaped geometry. The angle between the mean planes defined by the five-membered rings amounts to 111.5° (**3**) and 110.8° (**4**). The distance between the carbonyl O-atoms amounts to 5.76 Å (**3**) and 5.58 Å (**4**). The dihedral angle between the ipso carbons of the phenyl rings amounts to 28.7° (**3**) and 14.4° (**4**). Compound **3** is among the most twisted glycoluril derivatives reported to date.[29,38]

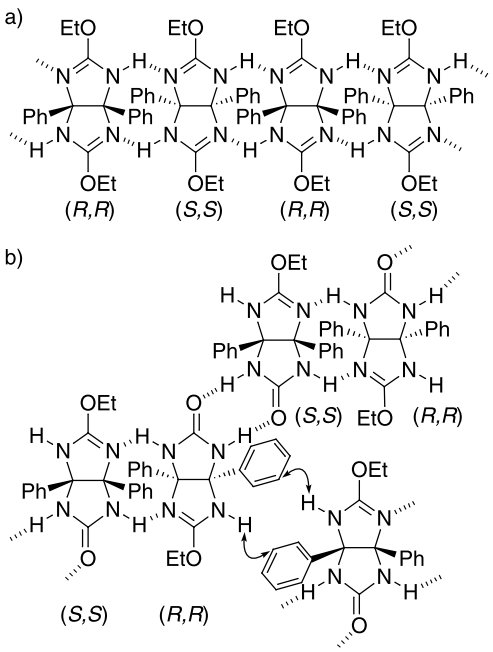

Figure 4. Schematic representations of the connectivity observed in H-bonded tapes of: (a) (±)-**1** and (b) (±)-**2**. The double headed arrow identifies a close contact between the unsatisfied H-bond donor N–H group and the adjacent phenyl ring indicative of an NH···π H-bond.

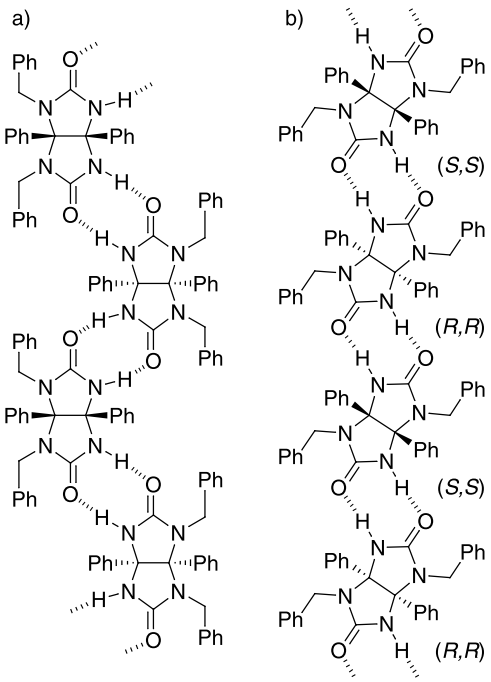

Figure 5. Schematic representations of the connectivity observed in H-bonded tapes of: (a) **3** and (b) (±)-**4**.

2.4. Hydrogen bond mediated self-association in the solid state

Figs. 4 and 5 show schematic representations of H-bonded tapes that are observed in the solid state structures of **1**–**4**. The geometrical parameters of the hydrogen bonds in these tapes are unremarkable (Table 1).[44]

Compound **1** possesses two NH groups and two C=N H-bond acceptor groups. The spatial arrangement of these groups dictates the formation of $R_2^2(8)$ H-bonding motifs by the formation of two N–H···N H-bonds (Fig. 4(a)). The relative orientation of the phenyl groups on the convex face of the molecule between the two H-bonded molecules is determined by the chirality of the monomer. For example, the homochiral aggregation of two molecules of (*R*,*R*)-**1** or two molecules of (*S*,*S*)-**1** by H-bonding produces a dimer where all four phenyl rings are displayed on the same face of the aggregate. In theory, this process of enantiomeric self-recognition would terminate in the cyclization to form H-bonded cucurbit[*n*]uril analogs $\mathbf{1}_n$.[45] In the crystal, however, we observe the formation of H-bonded tapes formed exclusively by heterochiral recognition processes. The chirality of the monomers in the H-bonded tapes alternates (e.g. (*R*,*R*)-**1**·(*S*,*S*)-**1**) as shown in Fig. 4(a). This alternation of chirality results in two phenyl rings being

Table 1. Geometrical parameters of the H-bonds found in tapes of **1**–**4**

Compound	N···N (Å)	N–H···N (°)	N···O (Å)	N–H···O (°)
1	2.899(2)	172(2)		
	2.905(2)	172(2)		
2	2.9327(14)	165.1(14)	2.8282(13)	175.1(15)
3			2.895(3)	164(3)
			2.857(3)	164(2)
4			2.8165(19)	175(2)

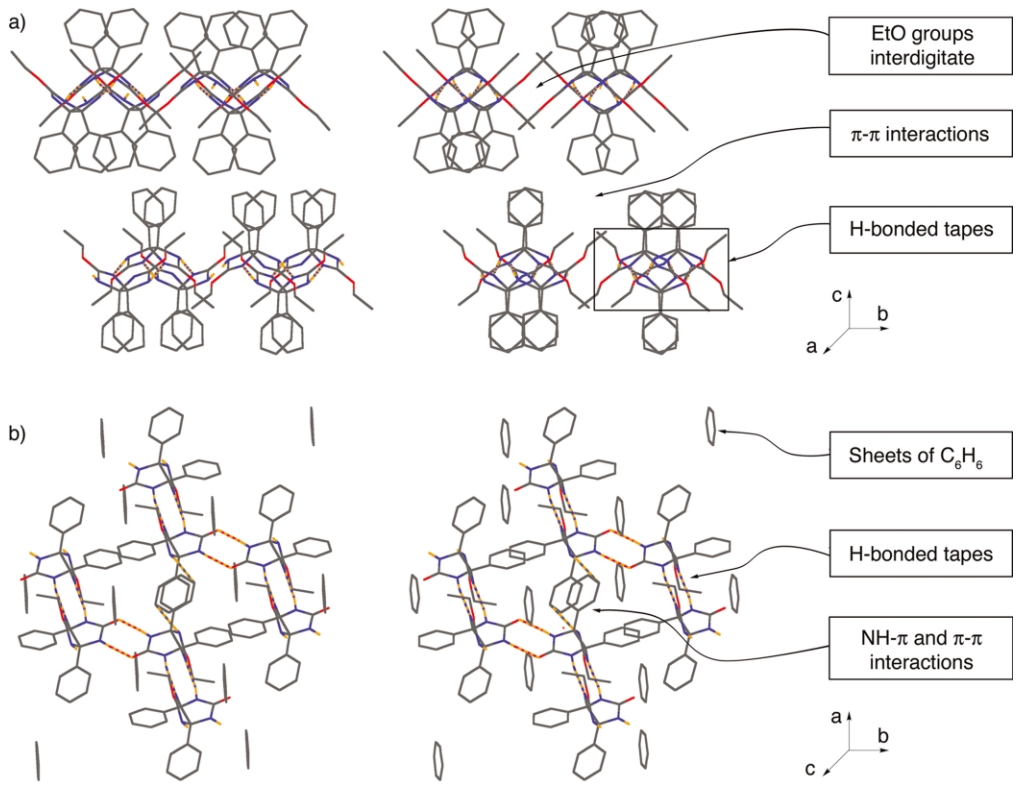

Figure 6. Cross-eyed stereoviews of the X-ray crystal structures of: (a) (±)-**1** viewed along the *a*-axis, and (b) (±)-**2**·$(C_6H_6)_{0.5}$ viewed along the *c*-axis. C: grey; H: orange; N: dark blue; O: red; H-bonds: striped. Hydrogen atoms not involved in hydrogen bonds have been omitted for clarity. The arrows highlight important aspects of the three-dimensional packing.

displayed on one face of the dimer and two on the other. Repetition of this process leads to a linear aggregate in the form of a hydrogen-bonded tape.

Compound (±)-**2** also crystallizes in the form of H-bonded tapes (Fig. 4(b)). The situation is far more complicated in this case, however, due to chirality, the presence of two distinct H-bonding faces, and the imbalance in the number of H-bond donors and acceptors.[12] In practice, heterochiral aggregation is observed exclusively. For example, the H-bonded tape shown in Fig. 4(b) can be built up by the heterochiral self-association of (*R*,*R*)-**2** and (*S*,*S*)-**2** by the formation of two N–H···N hydrogen bonds to yield the achiral *meso* building block (*R*,*R*)-**2**·(*S*,*S*)-**2**. Despite its achiral nature, the two ureidyl groups of (*R*,*R*)-**2**·(*S*,*S*)-**2** are enantiotopic. This dimeric building block then undergoes a second level of heterochiral oligomerization by formation of two N–H···O=C H-bonds between ureidyl groups of alternating topicity to form standard amide type dimeric eight-membered rings. The result of this heterochiral recognition process is the creation of the H-bonded tape shown in Fig. 4(b) in which the phenyl rings are displayed on alternating faces of the tape by the formation of two different $R_2^2(8)$ motifs.

Fig. 5 shows schematic representations of H-bonded tapes formed by **3** and (±)-**4** based on their X-ray crystal structures. Despite the fact that **3** is achiral, its ureidyl groups are enantiotopic. Therefore, the self-association of **3** can theoretically produce two dimeric aggregates that are diastereomers—one with all four phenyl substituents on one face of the dimer, the other has two on one face and two on the other as depicted (Fig. 5(a)). In each case, the dimerization occurs by the formation of two N–H···O H-bonds to yield the $R_2^2(8)$ H-bonding motif commonly observed in the crystal structures of amides. Further oligomerization by alternation of the phenyl rings leads to the observed H-bonded tape. The alternative mode of aggregation in which all phenyl groups are displayed on one side of the molecule would lead to the cyclic structure $\mathbf{3}_n$. We do not observe these types of structures for **3** either in solid state or in solution likely due to the efficient packing of the tapes in the solid state and an insufficient number of hydrogen bonds to overcome the unfavourable entropy associated with the formation of $\mathbf{3}_n$ in solution.[46,47] We note, however, that this pattern of H-bonds can be enforced by covalent connection of the glycoluril rings as has been beautifully demonstrated by Rebek in the formation of H-bonded capsules.[2,40]

Fig. 5(b) shows a schematic representation of the $R_2^2(8)$ H-bonded motif formed by (±)-**4** in the solid state. Similar to (±)-**1**, the aggregation of (±)-**4** can occur by either a homochiral ((*R*,*R*)-$\mathbf{4}_n$ and (*S*,*S*)-$\mathbf{4}_n$) or a heterochiral recognition process. In practice, we observe the formation of H-bonded tapes by the heterochiral recognition process in which molecules of (*R*,*R*)-**4** H-bond exclusively with molecules of (*S*,*S*)-**4** and vice versa through the formation of eight-membered H-bonded rings. This alternation of chirality places the phenyl substituents on opposing sides of the H-bonded tape. The hypothetical homochiral recognition process would generate a H-bonded helix.[48]

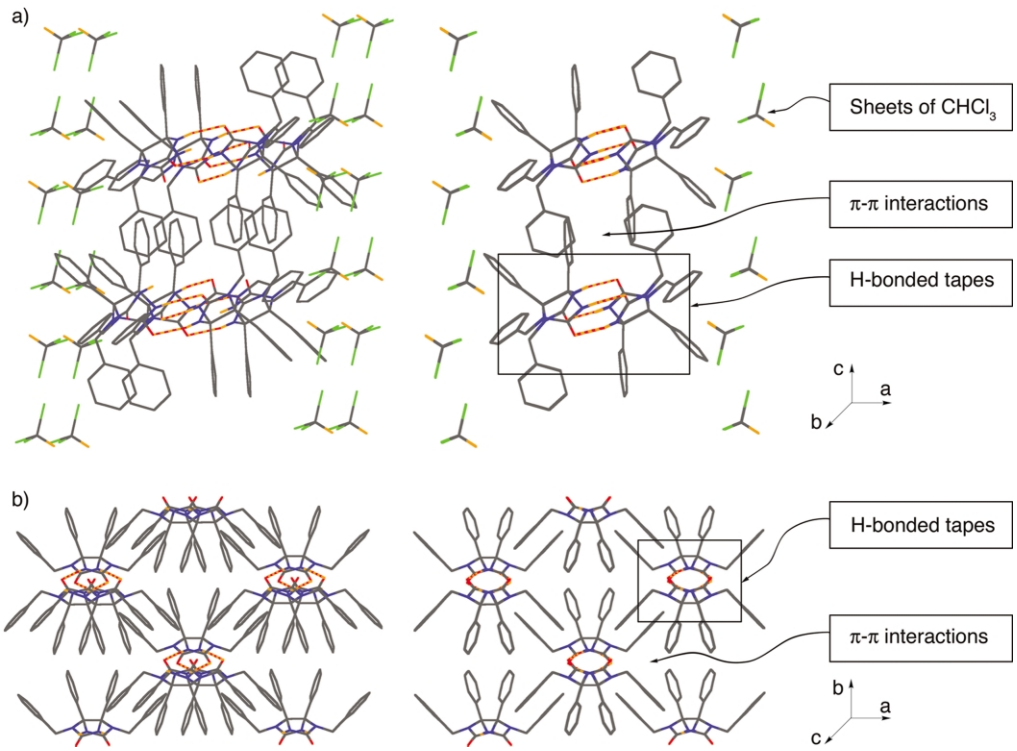

Figure 7. Cross-eyed stereoviews of the X-ray crystal structures of: (a) **3**·$CHCl_3$ viewed along the *b*-axis, and (b) (±)-**4** viewed along the *c*-axis. C: grey; H: orange; Cl: light green; N: dark blue; O: red; H-bonds: striped. Hydrogen atoms not involved in hydrogen bonds have been omitted for clarity. The arrows highlight important aspects of the three-dimensional packing.

2.5. Packing of the hydrogen bonded tapes in the crystal

Compounds **1**–**4** form tapes by the formation of H-bonded eight-membered rings. Conceptually, a three-dimensional solid can then be built up by the packing of these tapes in a variety of manners. Fig. 6 shows stereoscopic representations of the crystal structures of (±)-**1** and (±)-**2**. As described above, (±)-**1** forms H-bonded tapes in the crystal; Fig. 6(a) shows a view down the *a*-axis of the crystal which corresponds to the long axis of the tape. As can be readily seen from Fig. 6(a), the tapes of (±)-**1** pack in the crystal with their long axes parallel to one another. This three-dimensional packing is facilitated along the *b*-axis by the interdigitation of the OCH_2CH_3 groups. Along the *c*-axis, the predominant mode of interaction involves the phenyl rings forming favorable π−π interactions.[49] An examination of the geometry of these interactions reveals the predominant formation of T-shaped edge-to-face type interactions.[50] The three-dimensional packing of (±)-**2** is more complex. The tape grows along the *ab*-diagonal by the formation of H-bonded eight-membered rings between molecules of **2** of alternating chirality as shown (Fig. 6(b)). Similar to the packing of **1**, tapes of **2** pack with their long axes parallel to one another. In the case of **2**, however, the formation of NH···π interactions[51] appears to promote the alignment of the tapes along the *ab*-axis. As shown schematically (Fig. 4(b)), the unsatisfied H-bond donating NH group adjacent to the OEt group forms a close contact with one of the C-atoms on the phenyl ring of the adjacent tape. In return, the unsatisfied NH group on this adjacent molecule forms an identical close contact with the phenyl ring of the original molecule. Layers of solvating PhH delineate the boundaries of the sheets comprising the H-bonded tapes. The growth of the H-bonded tapes occurs alternately along the *ab*-axis and along the *ab*-diagonal as one moves along the *c*-axis. Order along the *c*-axis is promoted by the presence of sheets of solvating PhH rings. An examination of the geometry of the interacting aromatic rings reveals that each PhH ring interacts with phenyl rings of two molecules of **2** with a T-shaped geometry.

Fig. 7 shows stereoviews of the packing of the tapes formed by **3** and (±)-**4** in three dimensions. Similar to **1**, the tapes of **3** align with their long axes parallel to one another along the *b*-axis (Fig. 7(a)). Ordering along the *c*-axis is promoted by π−π interactions between the tapes. Examination of the geometry of the interacting phenyl rings reveals both offset face-to-face π-stacking and T-shaped edge-to-face type interactions. This ordering along the *c*-axis results in slabs of H-bonded tapes. These slabs of H-bonded tapes do not interact with one another in a direct fashion along the *a*-axis. Rather, layers of solvating $CHCl_3$ molecules interact with the phenyl rings on the sides of the slabs through C–H···π interactions.[52] Just like **3**, the tapes formed by (±)-**4** align with their long axes parallel to one another, in this case along the *c*-axis. The three-dimensional ordering of these tapes along the *a*- and *b*-axes is, once again promoted by π–π interactions. In this case, both phenyl substituents on the convex face of the glycoluril interact in an edge-to-face type manner with the benzyl groups on the opposing molecules.

3. Conclusion

In summary, we have presented the synthesis and X-ray crystal structures of alkylated glycoluril derivatives (±)-**1**,

(±)-**2**, **3**, and (±)-**4**. In contrast to the known crystal structures of glycoluril derivatives, all four compounds form H-bonded tapes in the crystal by the formation of $R_2^2(8)$ hydrogen bonding motifs. This tape forming process is the result of exclusive heterochiral recognition processes within the tapes. The alternative homochiral recognition processes that would lead to cyclic tapes—congeners of cucurbit-[*n*]uril—are not observed. We attribute the high propensity of **1**–**4** to form tapes to the use of phenyl and benzyl substituents which impart good solubility characteristics in non-polar aprotic solvents. These non-polar aprotic solvents do not compete for H-bonds with the ureidyl groups and that results in the predictable formation of H-bonded tapes. Collectively, the results presented in this paper suggest that glycoluril derivatives have significant potential as a building block in studies of crystal engineering.

4. Experimental

4.1. General

Starting materials were purchased from Alfa-Aesar, Acros, and Aldrich and were used without further purification. Compound **5c** was prepared according to the literature procedure.[53] TLC analysis was performed using pre-coated glass plates from Analtech or E. Merck. Column chromatography was performed using silica gel (230–400 mesh, 0.040–0.063 μm) from E. Merck using eluents in the indicated v:v ratio. Melting points were measured on a Meltemp apparatus in open capillary tubes and are uncorrected. IR spectra were recorded on a Nicolet Magna spectrophotometer as KBr pellets or thin films on NaCl plates and are reported in cm^{-1}. NMR spectra were measured on Bruker AM-400 and DRX-400 instruments operating at 400 MHz for ^1H and 100 MHz for ^{13}C. Mass spectrometry was performed using a VG 7070E magnetic sector instrument by electron impact (EI) or by fast atom bombardment (FAB) using the indicated matrix. The matrix 'magic bullet' is a 5:1 (w:w) mixture of dithiothreitol/dithioerythritol. Elemental analyses were performed by Midwest MicroLab (Indianapolis, IN).

4.2. Synthesis and characterization of 1–4

4.2.1. Compounds 1 and 2. A mixture of **5c** (2.94 g, 10.0 mmol) and Et_3OBF_4 (3.80 g, 20.0 mmol) in $ClCH_2$-CH_2Cl (10 mL) was heated at reflux under N_2 for 2 days while being stirred vigorously. The reaction mixture was quenched with aq. K_2CO_3 (50% sat., 50 mL), extracted with $CHCl_3$ (2×250 mL), dried over anhydrous K_2CO_3 and concentrated. The residue was washed with EtOAc (2 mL), centrifuged, and the supernatant decanted leaving a crude white solid. Flash chromatography (SiO_2, $CHCl_3$/MeOH 50:1) gave **1** (186 mg, 5%) and **2** (715 mg, 22%) as white solids.

Compound **1**.[42] Mp 241–242°C. TLC ($CHCl_3$/MeOH 25:1) R_f 0.37. IR (KBr, cm^{-1}): 3381w, 3064s, 2902m, 2828m, 1626s, 1582m, 1498s, 1471m, 1378m, 1332s, 1229m, 1081m, 1038s. ^1H NMR (400 MHz, DMSO-d_6): 7.32 (br s, 2H), 7.05–7.00 (m, 4H), 7.00–6.85 (m, 6H), 4.31 (br s, 4H), 1.33 (t, J=7.0 Hz, 6H). ^{13}C NMR (100 MHz, DMSO-d_6): 166.4, 142.1, 127.7, 127.6, 127.2, 95.9, 64.8, 15.5. MS (EI): *m/z* 350 (100, M^+). HR-MS (EI): *m/z* 350.1735 (M^+, $C_{20}H_{22}N_4O_2$, calcd 350.1743).

Compound **2**. Mp 250–251°C. TLC ($CHCl_3$/MeOH 25:1) R_f 0.13. IR (KBr, cm^{-1}): 3425m, 3176s, 2988w, 1720s, 1606s, 1518m, 1449m, 1374m, 1332s, 1227m, 1024m. ^1H NMR (400 MHz, DMSO-d_6): 7.64 (s, 1H), 7.53 (s, 1H), 7.47 (s, 1H), 7.05–6.85 (m, 10H), 4.40–4.25 (m, 2H), 1.33 (t, J=7.0 Hz, 3H). ^{13}C NMR (100 MHz, DMSO-d_6): 164.6, 161.3, 140.4, 139.2, 127.2, 127.1, 126.8, 91.6, 85.6, 64.1, 14.5 (14 resonances expected, 11 found). MS (FAB, Magic Bullet): *m/z* 323 (100, $[M+H]^+$). HR-MS (FAB, Magic Bullet): *m/z* 323.1508 ($[M+H]^+$, $C_{18}H_{19}N_4O_2$, calcd 323.1518).

4.2.2. Compounds 3 and 4. A mixture of **6** (31.5 g, 0.21 mol) and **7** (22.0 g, 0.105 mol) was dissolved in EtOH (210 mL) with heating. The homogenous solution was saturated with HCl gas and heated at reflux for 20 h. The reaction mixture was cooled to room temperature, filtered, and the solid was washed with EtOH. The crude solid (22.0 g) was chromatographed (SiO_2, $CHCl_3$/MeOH 50:1 to 9:1) in 4 g portions yielding *cis*-**1** (10.0 g, 20%) and *trans*-**1** (10.0 g, 20%) as white solids.

Compound **3**. Mp 289–290°C. TLC ($CHCl_3$/MeOH 50:1) R_f 0.11. IR (KBr, cm^{-1}): 3395w, 3216m, 3090w, 3063w, 2925w, 1716s, 1688s, 1467m, 1448s. ^1H NMR (400 MHz, DMSO-d_6): 8.40 (s, 2H), 7.30–7.00 (m, 16H), 6.93 (t, J=7.8 Hz, 2H), 6.65 (d, J=7.8 Hz, 2H), 4.36 (d, J=16.8 Hz, 2H), 3.84 (d, J=16.8 Hz, 2H). ^{13}C NMR (100 MHz, DMSO-d_6): δ 160.2, 139.0, 137.1, 132.9, 128.7, 128.2, 128.2, 128.0, 127.9, 127.6, 127.1, 126.6, 126.5, 90.3, 79.6, 44.7. MS (FAB, glycerol+TFA): *m/z* 475 (4, $[M+H]^+$), 91 (100, $C_7H_7^+$). HR-MS (FAB, glycerol+TFA): *m/z* 475.2087 ($[M+H]^+$, $C_{30}H_{27}N_4O_2$, calcd 475.2134).

Compound (±)-**4**. Mp 332–334°C. TLC ($CHCl_3$/MeOH 50:1) R_f 0.33. IR (KBr, cm^{-1}): 3418m, 3193m, 3084m, 3066m, 2922w, 2863w, 1716s, 1692s, 1474s, 1450s. ^1H NMR (400 MHz, DMSO-d_6): δ 8.43 (s, 2H). 7.30–6.95 (m, 20H), 4.49 (d, J=16.2 Hz, 2H), 3.86 (d, J=16.2 Hz, 2H). ^{13}C NMR (100 MHz, DMSO-d_6): δ 159.0, 139.0, 135.1, 128.4, 127.9, 127.8, 127.2, 127.1, 126.5, 84.7, 43.9. MS (FAB, glycerol+TFA): *m/z* 475 (23, $[M+H]^+$), 91 (100, $C_7H_7^+$). HR-MS (FAB, glycerol+TFA): *m/z* 475.2117 ($[M+H]^+$, $C_{30}H_{27}N_4O_2$, calcd 475.2134). Anal. calcd for $C_{30}H_{26}N_4O_2$ (474.55): C 75.93, H 5.52. Found: C 76.01, H 5.53.

4.3. X-Ray crystallographic analyses

Crystallographic data for the structures reported in this paper have been deposited with the Cambridge Crystallographic Data Centre as supplementary publication no. CCDC-192264 (**1**), CCDC-192265 (**2**), CCDC-192266 (**3**), and CCDC-192267 (**4**). Copies of the data can be obtained free of charge on application to CCDC, 12 Union Road, Cambridge CB2 1EZ, UK (fax: +44-1223-336-033; e-mail: deposit@ccdc.cam.ac.uk).

4.3.1. Crystal data for 1. $C_{20}H_{22}N_4O_2$, M=350.42, T=193(2) K, crystal system orthorhombic, space group *Fdd*2, a=9.8463(3) Å, b=17.6634(5) Å, c=44.8679(13) Å,

α=90°, β=90°, γ=90°, V=7803.4(4) Å^3, Z=16, ρ_{calcd}=1.193 g cm^{-3}, μ=0.079 mm^{-1}, F(000)=2976, crystal dimensions 0.562×0.280×0.102 mm^3, θ-range 1.82–27.50°, index ranges $-12\leq h\leq 12$, $-22\leq k\leq 22$, $-58\leq l\leq 58$, N_{tot}=30067, N_{indep}=4491 (R_{int}=0.0310), data/restraints/parameters=4491/1/325, GOF on F^2=1.072, final R indices [$I>2\sigma(I)$]: $R1$=0.0.0410, $wR2$=0.1071, R indices (all data): $R1$=0.0532, $wR2$=0.1150, largest diff. peak and hole 0.218 and −0.185 e Å^{-3}.

4.3.2. Crystal data for 2. $C_{21}H_{21}N_4O_2$, M=361.42, T=193(2) K, crystal system monoclinic, space group $C2/c$, a=12.6833(7) Å, b=14.6934(8) Å, c=20.0209(11) Å, α=90°, β=95.5590(10)°, γ=90°, V=3713.6(4) Å^3, Z=8, ρ_{calcd}=1.293 g cm^{-3}, μ=0.086 mm^{-1}, F(000)=1528, crystal dimensions 0.491×0.291×0.245 mm^3, θ-range 2.04–27.49°, index ranges $-16\leq h\leq 16$, $-19\leq k\leq 19$, $-25\leq l\leq 25$, N_{tot}=28955, N_{indep}=4274 (R_{int}=0.0274), data/restraints/parameters=4274/0/329, GOF on F^2=1.086, final R indices [$I>2\sigma(I)$]: $R1$=0.0400, $wR2$=0.0990, R indices (all data): $R1$=0.0530, $wR2$=0.1068, largest diff. peak and hole 0.254 and −0.206 e Å^{-3}.

4.3.3. Crystal data for 3. $C_{31}H_{27}Cl_3N_4O_2$, M=593.92, T=153(2) K, crystal system monoclinic, space group $P2(1)/c$, a=15.6468(11) Å, b=10.8710(9) Å, c=17.0339(9) Å, α=90°, β=95.532(5)°, γ=90°, V=2883.9(3) Å^3, Z=4, ρ_{calcd}=1.368 g cm^{-3}, μ=0.354 mm^{-1}, F(000)=1232, crystal dimensions 0.500×0.375×0.050 mm^3, θ-range 2.23–24.98°, index ranges $-18\leq h\leq 18$, $-12\leq k\leq 12$, $-20\leq l\leq 20$, N_{tot}=10511, N_{indep}=5064 (R_{int}=0.0650), data/restraints/parameters=5064/1/503, GOF on F^2=0.978, final R indices [$I>2\sigma(I)$]: $R1$=0.0487, $wR2$=0.0955, R indices (all data): $R1$=0.1053, $wR2$=0.1124, largest diff. peak and hole 0.245 and −0.274 e Å^{-3}.

4.3.4. Crystal data for 4. $C_{30}H_{26}N_4O_2$, M=474.55, T=193(2) K, crystal system monoclinic, space group $C2/c$, a=16.241(3) Å, b=12.987(2) Å, c=11.8330(19) Å, α=90°, β=98.872(3)°, γ=90°, V=2466.0(7) Å^3, Z=4, ρ_{calcd}=1.278 g cm^{-3}, μ=0.082 mm^{-1}, F(000)=1000, crystal dimensions 0.686×0.245×0.220 mm^3, θ-range 2.02–27.50°, index ranges $-21\leq h\leq 21$, $-16\leq k\leq 16$, $-14\leq l\leq 15$, N_{tot}=2795, N_{indep}=2795 (R_{int}=0.0000), data/restraints/parameters=2795/0/221, GOF on F^2=1.124, final R indices [$I>2\sigma(I)$]: $R1$=0.0465, $wR2$=0.1470, R indices (all data): $R1$=0.0570, $wR2$=0.1576, largest diff. peak and hole 0.279 and −0.189 e Å^{-3}.

Acknowledgements

We thank the National Institutes of Health (GM61854) for generous financial support. L. I. is a Cottrell Scholar of Research Corporation.

References

1. (a) Jacobs, W.; Foster, D.; Sansur, S.; Lees, R. G. *Prog. Org. Coat.* **1996**, *29*, 127–138. (b) Parekh, G. G. US Patent 4,105,708, 1978. (c) Wang, A.; Bassett, D. US Patent 4,310,450, 1982. (d) Yinon, J.; Bulusu, S.; Axenrod, T.; Yazdekhasti, H. *Org. Mass Spectrom.* **1994**, *29*, 625–631. (e) Boileau, J.; Carail, M.; Wimmer, E.; Gallo, R.; Pierrot, M. *Propellants, Explos., Pyrotech.* **1985**, *10*, 118–120. (f) Krause, A.; Aumueller, A.; Korona, E.; Trauth, H. US Patent 5,670,613, 1997. (g) Karcher, S.; Kornmuller, A.; Jekel, M. *Water Sci. Technol.* **1999**, *40*, 425–433. (h) Pryor, K. E.; Rebek, Jr. J. *Org. Lett.* **1999**, *1*, 39–42.
2. Hof, F.; Craig, S. L.; Nuckolls, C.; Rebek, Jr. J. *Angew. Chem. Int. Ed.* **2002**, *41*, 1488–1508.
3. Rowan, A. E.; Elemans, J. A. A. W.; Nolte, R. J. M. *Acc. Chem. Res.* **1999**, *32*, 995–1006.
4. (a) Sun, S.; Harrison, P. *Tetrahedron Lett.* **1992**, *33*, 7715–7718. (b) Sun, S.; Harrison, P. *J. Chem. Soc., Chem. Commun.* **1994**, 2235–2236.
5. (a) Isaacs, L.; Witt, D.; Lagona, J. *Org. Lett.* **2001**, *3*, 3221–3224. (b) Isaacs, L.; Witt, D. *Angew. Chem. Int. Ed.* **2002**, *41*, 1905–1907.
6. Kölbel, M.; Menger, F. M. *Chem. Commun.* **2001**, 275–276.
7. (a) Kim, J.; Jung, I.-S.; Kim, S.-Y.; Lee, E.; Kang, J.-K.; Sakamoto, S.; Yamaguchi, K.; Kim, K. *J. Am. Chem. Soc.* **2000**, *122*, 540–541. (b) Freeman, W. A.; Mock, W. L.; Shih, N. Y. *J. Am. Chem. Soc.* **1981**, *103*, 7367–7368. (c) Day, A.; Arnold, A. P.; Blanch, R. J.; Snushall, B. *J. Org. Chem.* **2001**, *66*, 8094–8100.
8. Kurth, D. G.; Fromm, K. M.; Lehn, J.-M. *Eur. J. Inorg. Chem.* **2001**, 1523–1526.
9. Etter, M. C. *Acc. Chem. Res.* **1990**, *23*, 120–126.
10. Etter, M. C. *J. Phys. Chem.* **1991**, *95*, 4601–4610.
11. Zerkowski, J. A.; MacDonald, J. C.; Seto, C. T.; Wierda, D. A.; Whitesides, G. M. *J. Am. Chem. Soc.* **1994**, *116*, 2382–2391.
12. Brienne, M.-J.; Gabard, J.; Leclercq, M.; Lehn, J.-M.; Cesario, M.; Pascard, C.; Chevé, M.; Dutruc-Rosset, G. *Tetrahedron Lett.* **1994**, *35*, 8157–8160.
13. Palmore, G. T. R.; Luo, T.-J. M.; McBride-Wieser, M. T.; Picciotto, E. A.; Reynoso-Paz, C. M. *Chem. Mater.* **1999**, *11*, 3315–3328.
14. Palacin, S.; Chin, D. N.; Simanek, E. E.; MacDonald, J. C.; Whitesides, G. M.; McBride, M. T.; Palmore, G. T. R. *J. Am. Chem. Soc.* **1997**, *119*, 11807–11816.
15. McBride, M. T.; Luo, T.-J. M.; Palmore, G. T. R. *Cryst. Growth Des.* **2001**, *1*, 39–46.
16. Simanek, E. E.; Tsoi, A.; Wang, C. C. C.; Whitesides, G. M.; McBride, M. T.; Palmore, G. T. R. *Chem. Mater.* **1997**, *9*, 1954–1961.
17. MacDonald, J. C.; Whitesides, G. M. *Chem. Rev.* **1994**, *94*, 2383–2420.
18. Meléndez, R. E.; Hamilton, A. D. *Top. Curr. Chem.* **1998**, *198*, 97–129.
19. Li, N.; Maluendes, S.; Blessing, R. H.; Dupuis, M.; Moss, G. R.; DeTitta, G. T. *J. Am. Chem. Soc.* **1994**, *116*, 6494–6507.
20. Xu, S.; Gantzel, P. K.; Clark, L. B. *Acta Crystallogr., Sect. C* **1994**, *C50*, 1988–1989.
21. Modric, N.; Poje, M.; Vickovic, I. *Acta Crystallogr., Sect. C* **1995**, *51*, 2594–2595.
22. Himes, V. L.; Hubbard, C. R.; Mighell, A. D.; Fatiadi, A. J. *Acta. Crystallogr., Sect B* **1978**, *B34*, 3102–3104.
23. (a) Flippen-Anderson, J. L.; Kony, M.; Dagley, I. J. *Acta Crystallogr., Sect. C* **1994**, *C50*, 974–976. (b) Boileau, J.; Wimmer, E.; Pierrot, M.; Baldy, A.; Gallo, R. *Acta Crystallogr., Sect. C* **1985**, *C41*, 1680–1683. (c) Boileau, J.;

Wimmer, E.; Gilardi, R.; Stinecipher, M. M.; Gallo, R.; Pierrot, M. *Acta Crystallogr., Sect. C* **1988**, *C44*, 696–699.
24. (a) Bosman, W. P.; Smits, J. M. M.; de Gelder, R.; Reek, J. N. H.; Elemans, J. A. A. W.; Nolte, R. J. M. *J. Chem. Crystallogr.* **1997**, *27*, 75–79. (b) Bosman, W. P.; Smits, J. M. M.; de Gelder, R.; Reek, J. N. H.; Nolte, R. J. M. *J. Chem. Crystallogr.* **1996**, *26*, 365–368. (c) Holder, S. J.; Elemans, J. A. A. W.; Donners, J. J. J. M.; Boerakker, M. J.; de Gelder, R.; Barberá, J.; Rowan, A. E.; Nolte, R. J. M. *J. Org. Chem.* **2001**, *66*, 391–399. (d) Martens, C. F.; Sijbesma, R. P.; Klein Gebbink, R. J. M.; Spek, A. L.; Nolte, R. J. M. *Recl. Trav. Chim. Pays-Bas* **1993**, *112*, 400–403. (e) Reek, J. N. H.; Engelkamp, H.; Rowan, A. E.; Elemans, J. A. A. W.; Nolte, R. J. M. *Chem. Eur. J.* **1998**, *4*, 716–722. (f) Reek, J. N. H.; Rowan, A. E.; Crossley, M. J.; Nolte, R. J. M. *J. Org. Chem.* **1999**, *64*, 6653–6663. (g) Reek, J. N. H.; Rowan, A. E.; de Gelder, R.; Beurskens, P. T.; Crossley, M. J.; De Feyter, S.; de Schryver, F.; Nolte, R. J. M. *Angew. Chem. Int. Ed. Engl.* **1997**, *36*, 361–363. (h) Schenning, A. P. H. J.; de Bruin, B.; Rowan, A. E.; Kooijman, H.; Spek, A. L.; Nolte, R. J. M. *Angew. Chem. Int. Ed. Engl.* **1995**, *34*, 2132–2134. (i) Smeets, J. W. H.; Sijbesma, R. P.; van Dalen, L.; Spek, A. L.; Smeets, W. J. J.; Nolte, R. J. M. *J. Org. Chem.* **1989**, *54*, 3710–3717. (j) Sijbesma, R. P.; Kentgens, A. P. M.; Lutz, E. T. G.; van der Maas, J. H.; Nolte, R. J. M. *J. Am. Chem. Soc.* **1993**, *115*, 8999–9005. (k) Bosman, W. P.; Beurskens, P. T.; Admiraal, G.; Sijbesma, R. P.; Nolte, R. J. M. *Z. Kristallogr.* **1991**, *197*, 305–308. (l) Isaacs, L.; Witt, D.; Fettinger, J. C. *Chem. Commun.* **1999**, 2549–2550.
25. Garcias, X.; Toledo, L. M.; Rebek, Jr. J. *Tetrahedron Lett.* **1995**, *36*, 8535–8538.
26. Mock, W. L.; Manimaran, T.; Freeman, W. A.; Kuksuk, R. M.; Maggio, J. E.; Williams, D. H. *J. Org. Chem.* **1985**, *50*, 60–62.
27. Cow, C. N.; Britten, J. F.; Harrison, P. H. M. *Chem. Commun.* **1998**, 1147–1148.
28. Matta, C. F.; Cow, C. C.; Sun, S.; Britten, J. F.; Harrison, P. H. M. *J. Mol. Struct.* **2000**, *523*, 241–255.
29. Duspara, P. A.; Matta, C. F.; Jenkins, S. I.; Harrison, P. H. M. *Org. Lett.* **2001**, *3*, 495–498.
30. Geiling, G. T. W.; Nolte, R. J. M.; Scheeren, J. W.; Smits, I. M. M.; Beurskens, P. T.; Beurskens, G. *J. Chem. Crystallogr.* **1995**, *25*, 421–424.
31. Schouten, A.; Kanters, J. A. *Acta Crystallogr., Sect. C* **1990**, *C46*, 2484–2486.
32. Shamuratov, E. B.; Batsanov, A. S.; Struchkov, Y. T.; Tsivadze, A. Y.; Tsintsadze, M. G.; Khmel'nitskii, L. I.; Simonov, Y. A.; Dvorkin, A. A.; Lebedev, O. V.; Markova, T. B. *Chem. Heterocycl. Compd.* **1991**, *27*, 745–749.
33. Kostyanovsky, R. G.; Lyssenko, K. A.; Kravchenko, A. N.; Lebedev, O. V.; Kadorkina, G. K.; Kostyanovsky, V. R. *Mendeleev Commun.* **2001**, 134–136.
34. Sun, S.; Britten, J. F.; Cow, C. N.; Matta, C. F.; Harrison, P. H. M. *Can. J. Chem.* **1998**, *76*, 301–306.
35. Modric, N.; Poje, M.; Vickovic, I.; Bruvo, M. *Acta Crystallogr., Sect. C* **1990**, *C46*, 1336–1338.
36. Dekaprilevich, M. O.; Suvorova, L. I.; Khmelnitskii, L. I.; Struchkov, Y. T. *Acta Crystallogr., Sect. C* **1994**, *C50*, 2056–2058.
37. Tanaka, S.; Kato, K.; Kimoto, H.; Seguchi, K. *Anal. Sci.* **1999**, *15*, 817–818.
38. A report from the Rebek group describing the formation of H-bonded tapes in the X-ray crystal structures of derivatives of **3** appeared after submission of this manuscript. See: Johnson, D. W.; Palmer, L. C.; Hof, F.; Iovine, P. M.; Rebek, Jr. J. *Chem. Commun.* **2002**, 2228–2229.
39. (a) Witt, D.; Lagona, J.; Damkaci, F.; Fettinger, J. C.; Isaacs, L. *Org. Lett.* **2000**, *2*, 755–758. (b) Wu, A.; Chakraborty, A.; Witt, D.; Lagona, J.; Damkaci, F.; Ofori, M.; Chiles, J. K.; Fettinger, J. C.; Isaacs, L. *J. Org. Chem.* **2002**, *67*, 5817–5830. (c) Chakraborty, A.; Wu, A.; Witt, D.; Lagona, J.; Fettinger, J. C.; Isaacs, L. *J. Am. Chem. Soc.* **2002**, *124*, 8297–8306. (d) Wu, A.; Chakraborty, A.; Fettinger, J. C.; Flowers, II., R. A.; Isaacs, L. *Angew. Chem. Int. Ed.* **2002**, in press.
40. O'Leary, B. M.; Szabo, T.; Svenstrup, N.; Schalley, C. A.; Lützen, A.; Schäfer, M.; Rebek, Jr. J. *J. Am. Chem. Soc.* **2001**, *123*, 11519–11533.
41. Valdés, C.; Spitz, U. P.; Toledo, L. M.; Kubik, S. W.; Rebek, Jr. J. *J. Am. Chem. Soc.* **1995**, *117*, 12733–12745.
42. Gompper, R.; Schwarzensteiner, M.-L. *Angew. Chem. Int. Ed. Engl.* **1983**, *22*, 543–544.
43. Gieling, G. T. W.; Scheeren, H. W.; Israël, R.; Nolte, R. J. M. *Chem. Commun.* **1996**, 241–243.
44. Taylor, R.; Kennard, O. *Acc. Chem. Res.* **1984**, *17*, 320–326.
45. It is possible that different solvents or guest molecules could template the formation of the cyclic aggregates. We have not observe cyclic aggregates in $CDCl_3$, CD_2Cl_2, C_6D_6, or C_7D_8 solution alone or in the presence of adamantane, 1-adamantaneacetic acid, or cyclohexanecarboxylic acid. We have not searched for the presence of polymorphs of **1**–**4** by performing powder diffraction studies.
46. Mammen, M.; Simanek, E. E.; Whitesides, G. M. *J. Am. Chem. Soc.* **1996**, *118*, 12614–12623.
47. Whitesides, G. M.; Simanek, E. E.; Mathias, J. P.; Seto, C. T.; Chin, D.; Mammen, M.; Gordon, D. M. *Acc. Chem. Res.* **1995**, *28*, 37–44.
48. Kostyanovsky, R. G.; Lyssenko, K. A.; Kadorkina, G. K.; Lebedev, O. V.; Kravchenko, A. N.; Chervin, I. I.; Kostyanovsky, V. R. *Mendeleev Commun.* **1998**, 231–233.
49. (a) Burley, S. K.; Petsko, G. A. *Science* **1985**, *229*, 23–28. (b) Hunter, C. A. *Chem. Soc. Rev.* **1994**, 101–109. (c) Jorgensen, W. L.; Severence, D. L. *J. Am. Chem. Soc.* **1990**, *112*, 4768–4774.
50. We describe the geometry of these interactions as edge-to-face, but as is commonly observed the C–H bonds are oriented toward one or two C-atoms of the opposing aromatic ring.
51. (a) Adams, H.; Carver, F. J.; Hunter, C. A.; Osborne, N. J. *Chem. Commun.* **1996**, 2529–2530. (b) Adams, H.; Harris, K. D. M.; Hembury, G. A.; Hunter, C. A.; Livingstone, D.; McCabe, J. F. *Chem. Commun.* **1996**, 2531–2532. (c) Mons, M.; Dimicoli, I.; Tardivel, B.; Piuzzi, F.; Brenner, V.; Millié, P. *Phys. Chem. Chem. Phys.* **2002**, *4*, 571–576. (d) Tsuzuki, S.; Honda, K.; Uchimaru, T.; Mikami, M.; Tanabe, K. *J. Am. Chem. Soc.* **2000**, *122*, 11450–11458. (e) Allen, F. H.; Hoy, V. J.; Howard, J. A. K.; Thalladi, V. R.; Desiraju, G. R.; Wilson, C. C.; McIntyre, G. J. *J. Am. Chem. Soc.* **1997**, *119*, 3477–3480.
52. Desiraju, G. R. *Acc. Chem. Res.* **2002**, *35*, 565–573.
53. Butler, A. R.; Leitch, E. *J. Chem. Soc., Perkin Trans. 2* **1980**, 103–105.